J Nanopart Res (2014) 16:2684
DOI 10.1007/s11051-014-2684-8

RESEARCH PAPER

Conductive network structure formed by laser sintering of silver nanoparticles

Gang Qin · Akira Watanabe

Received: 16 March 2014 / Accepted: 29 September 2014 / Published online: 11 October 2014

Abstract The sintering of a silver (Ag) nanoparticle film by laser beam irradiation was studied using a CW DPSS laser. The laser sintering of the Ag nanoparticle thin film gave a transparent conductive film with a thickness of ca. 10 nm, whereas a thin film sintered by conventional heat treatment using an electronic furnace was an insulator because of the formation of isolated silver grains during the slow heating process. The laser sintering of the Ag nanoparticle thin film gave a unique conductive network structure due to the rapid heating and quenching process caused by laser beam scanning. The influences of the laser sintering conditions such as laser scan speed on the conductivity and the transparency were studied. With the increase of scan speed from 0.50 to 5.00 mm/s, the surface resistivity remarkably decreased from 4.45×10^8 to 6.30 Ω/sq. The addition of copper (Cu) nanoparticles to silver thin film was also studied to improve the homogeneity of the film and the conductivity due to the interaction between the oxidized surface of Cu nanoparticle and a glass substrate. By adding 5 wt% Cu nanoparticles to the Ag thin film, the surface resistivity improved to 2.40 Ω/sq.

G. Qin · A. Watanabe (✉)
Institute of Multidisciplinary Research for Advanced Materials, Tohoku University, Sendai 980-8577, Japan
e-mail: watanabe@tagen.tohoku.ac.jp

G. Qin
School of Materials Science and Engineering, Henan Polytechnic University, Jiaozuo 454001, China

Keywords Silver nanoparticles · Copper nanoparticles · Laser sintering · Conductive network structure · Transparent conductive film

Introduction

Recently, solution processes using various kinds of nano-materials are widely studied in the field of printed and flexible electronics (Ko et al. 2007a; Parka et al. 2007; Jeong et al. 2011; Singh et al. 2010; Ko et al. 2010; Woo et al. 2009) because a new manufacturing process which increases the productivity and reduces the energy consumption compared to conventional processes is desired. The reduction of environmental impact is also an important issue in developing the new manufacturing process. Metal nanoparticle is one of the important materials which can be applicable in many fields (Perelaer et al. 2006; Fuller et al. 2002; Yonezawa 2009; Tamai et al. 2008; Ko et al. 2007b). Inkjet printing technique using a metal nanoparticle ink is most widely studied in the field of printed and flexible electronics (Gamerith et al. 2007; Luechinger et al. 2008; Murata et al. 2005). In the inkjet printing process, metal nanoparticle-dispersed solution is jetted out on a substrate from a printer nozzle to draw metal nanoparticle micro-lines and the following heat treatment converts the insulating deposits of metal nanoparticles to conductive wiring. The heat treatment to sinter metal nanoparticles is conventionally carried out

using an electric furnace. In the process, the heat treatment of a whole substrate for several ten minutes is necessary to obtain a conductive wiring pattern. Laser processing has been applied to the sintering of metal nanoparticles to shorten the process time. In the previous papers, we have reported the silver (Ag) microwiring on a flexible polymer film by laser direct writing method using metal nanoparticle-dispersed ink (Aminuzzaman et al. 2008a, b, 2010). The sintering process by laser irradiation is efficient and fast process (Watanabe et al. 2005, 2007, 2012, 2013). The laser energy is efficiently absorbed by the plasmon resonance of metal nanoparticle in visible region. The confined energy in the thermally isolated metal nanoparticle with the size of several nanometers causes the rapid temperature rise and the efficient conversion of metal nanoparticles to a conductive metal film. The high special resolution of the laser processing is also advantageous compared to the conventional method. The linewidth of the Ag microwiring can be controlled flexibly by changing the objective lens characteristics, and then submicron Ag wiring was achieved with an objective lens with a high numerical aperture (N.A.) value (Watanabe et al. 2005, 2009). The laser processing has emerged as an attractive technique in microelectronics because of the fascinating features such as high resolution, high degree of flexibility to control the resolution and size of the micropatterns, high speed, and a little environmental pollution (Choi et al. 2004; Arnold et al. 2007; Piqué et al. 1999, 2008; Kim et al. 2004, 2007, 2010; Auyeung et al. 2009, 2011; Wang et al. 2010). In this paper, we applied the laser sintering to the fabrication of a transparent conductive metal film using Ag nanoparticles. Although the formation of a metal film with the thickness thinner than a few ten nanometers is required to obtain a transparent conductive film, there are a few studies on the formation of a transparent conductive film based on the solution process using metal nanoparticles. One of the difficulties in the formation of a thin metal film is the grain growth during the deposition of film, which induces the isolation of grains and the insulation of the film. In the case of the sintering of a thin film from metal nanoparticles using an electric furnace, the slow sintering process causes the grain growth, and then an island structure consisting of fused metal nanoparticles is formed. The faster sintering process is necessary to reduce the grain growth. Laser sintering is expected as an effective method to reduce the grain growth and enhance the conductivity of the film. Metal nanoparticles show an intense absorption band in visible region owing to the plasmon resonance. The laser irradiation to the nanoparticle causes the rapid temperature rise due to the efficient absorption of laser beam by the plasmon resonance of the metal nanoparticle and the confinement of the laser energy in thermally isolated metal nanoparticle with the size of several nanometers. The laser-irradiated metal nanoparticles work as a nano-heater and cause the rapid sintering (Watanabe et al. 2009).

Experimental

Materials

The Ag nanoparticle ink (Nanometal ink, Ag1T, average particle size ca. 4 nm) and copper (Cu) nanoparticle ink (Cu1T, average particle size ca. 4 nm) were purchased from ULVAC Technologies Inc. (ULVAC Inc. 2014). The Nanometal ink is produced by the gas evaporation method (gas-phase condensation) where Ag nanoparticles are individually dispersed in an organic solvent such as toluene. Nanoparticle surfaces were modified with organic surfactants to prevent agglomeration during preparation (Oda et al. 1992, 2001; Atsuki et al. 2004). The metal nanoparticle-dispersed films were prepared by spin-coating of the metal nanoparticle ink on a glass substrate at 2,000 rpm for 30 s and the obtained film was dried by heating at 110 °C for 30 s before laser irradiation.

Sintering

The diameter of the laser beam emitted from a CW DPSS laser (1,064 nm, 5 W, TEM_{00} Gaussian mode, CNI) was enlarged by a beam expander and then a line-shaped beam was obtained through a cylindrical lens. The experimental setup is illustrated in Fig. 1. The line-shaped beam was introduced into an optical microscope (BX-51M, OLYMPUS) and focused on the precursor film through an objective lens. Figure 2 shows the optical microscope image of the line-shaped beam during the scanning by PC-controlled xyz stage. Judging from the color change of Ag nanoparticle film, the length of the beam can be estimated to be ca. 400 μm. In the laser sintering experiments, the

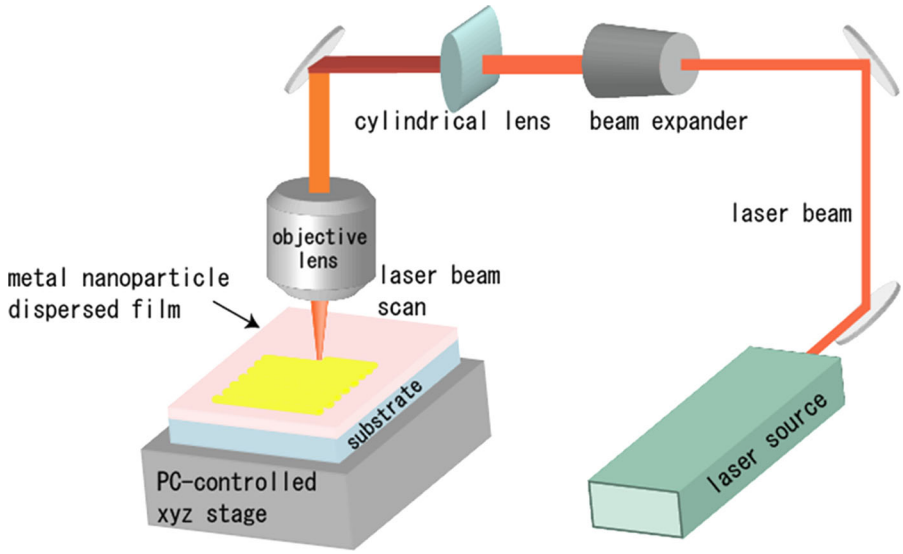

Fig. 1 Experimental setup of laser sintering

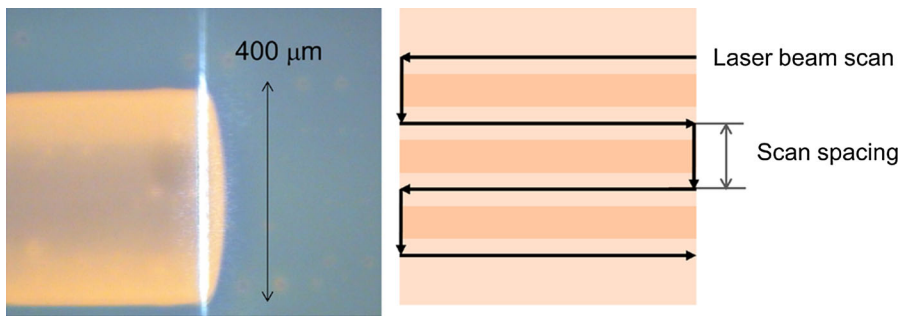

Fig. 2 Optical microscope image of the line-shaped laser beam during the scanning by the PC-controlled xyz stage and the scanning direction of the laser beam

optimized laser power was determined observing the change of the laser-irradiated area by the optical microscope. With increasing the laser power, the laser sintering took place above a critical laser power which was in the region of 2.2–2.5 W depending on the precursor film and the laser focusing conditions. Judging from the optical microscope view of the laser-irradiated area, the laser power of a minimum necessary value to cause the laser sintering is around 2.2 W. Because the critical laser power caused the instability in laser sintering, the laser power was set to 2.5 W with a margin of safety to cause the laser sintering. When the laser power was kept at 2.5 W, the change in the morphology and the resistivity of the laser-sintered film were not varied. The power density of the line-shaped laser beam was estimated to be 32 kW/cm^2 based on the optical microscope image of the laser beam as shown in Fig. 2. The laser scan spacing is defined by the width between laser scanning lines as shown in Fig. 2. The influence of the laser scan spacing is discussed in the latter section. The conventional sintering was carried out using an electric furnace at the heating rate of 20 °C/min.

Measurements

The surface morphology of the films was investigated by a scanning electron microscope (SEM, XL30, Philips Electronic N.V) and an analytical field emission SEM (FE-SEM SU6600, Hitachi). The surface resistivity was measured by a four-point probe method using a direct current voltage and current generator (6241A, ADCMT). Transmittance spectra were recorded by a UV–Vis/NIR spectrophotometer (V-670, JASCO). The thickness of a film was determined by interference method using a two beam interference objective lens (CF IC EPI PLAN DI 50XA, Nikon)

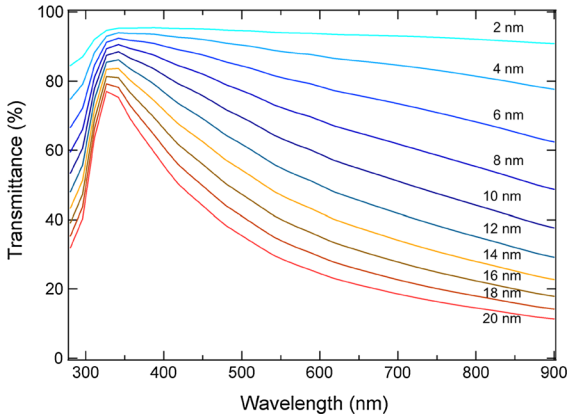

Fig. 3 Simulated transmission spectra of silver thin films

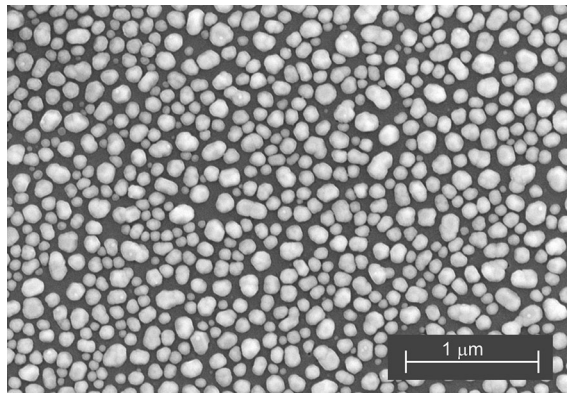

Fig. 4 SEM image of Ag nanoparticle film from 5 wt% Ag nanoparticle solution after heat treatment at 300 °C for 30 min in air

(Komatsu 1991). The simulation of the transmission spectra of silver thin films was carried out by a thin film analysis and design software (Film Wizard^{TM}, SCI).

Results and discussion

Sintering of Ag nanoparticle film

The transmittances of silver thin films were simulated based on the extinction coefficient and refractive index. Figure 3 shows the simulated transmission spectra of silver thin films whose thicknesses are in the range of 2–20 nm. A high transmittance is shown in the near UV region of 300 to 400 nm, where silver has a minimum refractive index. On the other hand, the transmittance decreases in the visible region with increasing the refractive index of silver and the thickness depending on the extinction coefficient at each wavelength. The surface resistivity of the transparent film in the practical use is required to be around 10 Ω/sq. The surface resistivity of the silver thin film with the thickness of 2 nm can be estimated to be 8.00 Ω/sq if the volume resistivity is assumed to be 1.6×10^{-6} Ω cm similar with the value of bulk silver. The surface resistivities of the all films simulated in Fig. 3 are low enough; however, the problem is the transparency in the visible region. To obtain transparency higher than 60 % at 550 nm, the thickness should be lower than 10 nm.

There are very few reports on the formation of a silver thin film by solution process. The thin film formation by the sintering of Ag nanoparticles has a problem of the grain formation. During the sintering of the nanoparticles, the grain growth is caused by the fusion and aggregation of Ag nanoparticles, which lead to a discontinuous island structure. The SEM image of the Ag nanoparticle film from 5 wt% toluene solution after heat treatment at 300 °C for 30 min in air is shown in Fig. 4. Although the film showed metallic color and high reflectance, the insulation was observed due to the discontinuous island structure. The grain growth must be caused by the slow sintering process by conventional heat treatment using an electronic furnace. The sintering time remarkably influenced the grain growth and the morphology. Figure 5 shows the SEM images of Ag nanoparticle films from 5 wt% solution after heat treatment at 250 °C for 5 and 10 min, where the sintering temperature was also lowered to reduce the grain growth. When the sintering time was shortened to 5 min, the shape of grains was not spherical as shown in Fig. 5a. With the increase of the sintering time to 10 min, the grain became spherical one as shown in Fig. 5c. The shape change of the grain was more clearly observed by the 45° tilt view. The SEM image of the film sintered for 5 min indicated the flat surface contact of grains with the surface of the substrate (Fig. 5b). On the other hand, the point contact of spherical grains with the substrate was observed as shown in Fig. 5d. The image of the grain growth and the influence of the sintering time are illustrated in Fig. 6. It was difficult to form a continuous sintered film even if the sintering time and temperature were decreased in the case of the

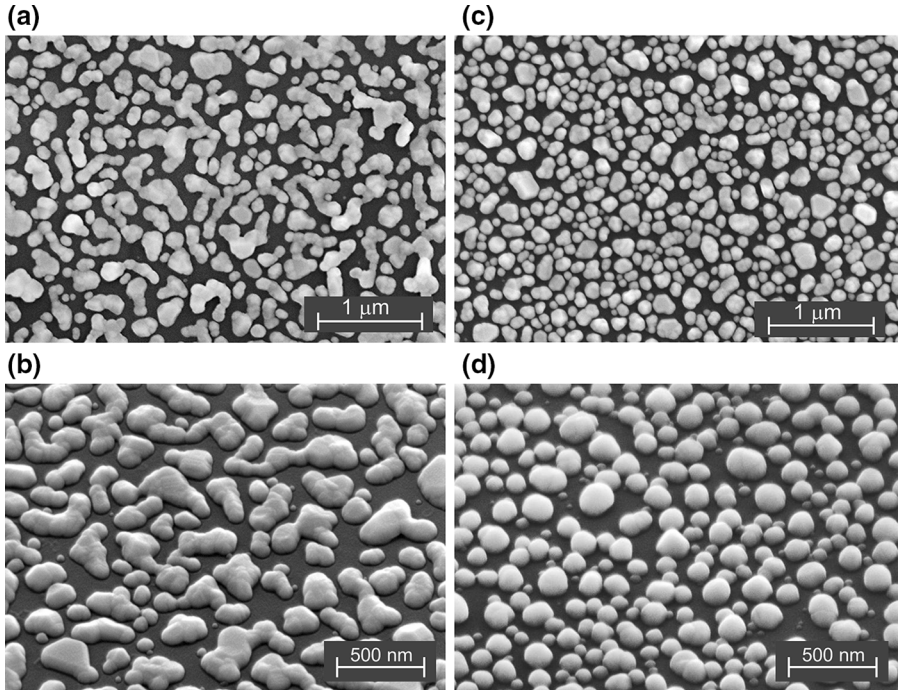

Fig. 5 SEM images of Ag nanoparticle films from 5 wt% Ag nanoparticle solution after heat treatment in air. **a** Top image after 5 min heating at 250 °C, **b** 45° tilt view after 5 min heating at 250 °C, **c** top image after 10 min heating at 250 °C, **d** 45° tilt view after 10 min heating at 250 °C

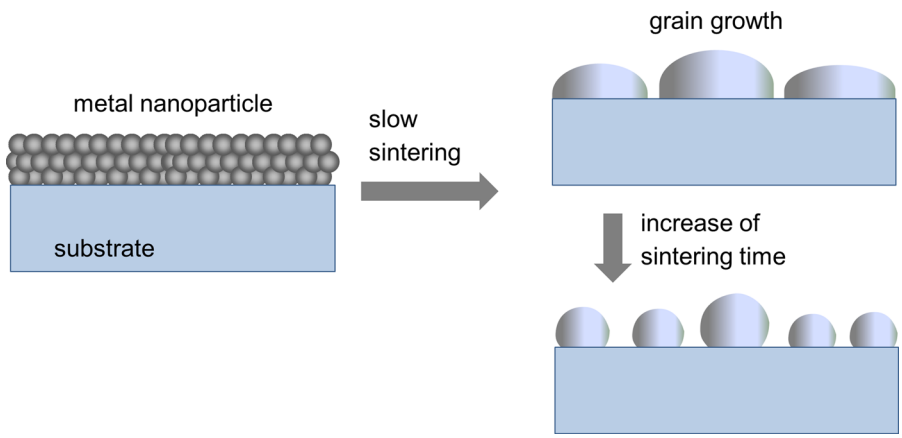

Fig. 6 Image of grain formation during the sintering of metal nanoparticles by conventional heat treatment using an electric furnace

conventional heat treatment. The films sintered at 250 °C for 5 and 10 min were insulators.

The reduction of the grain growth is expected by applying the laser sintering because the advantage of the laser sintering is the faster processing time compared to conventional methods. One of the factors to control the sintering of Ag nanoparticle film is the scan speed of laser beam. The surface resistivities of Ag nanoparticle laser-sintered films under different scan speeds are summarized in Table 1. With the increasing scan speed from 0.50 to 5.00 mm/s, the surface resistivity remarkably decreased from 4.45×10^8 to 6.30 Ω/sq. Both the films have an average thickness ca. 10 nm after laser sintering, which was determined by interference method using a two beam interference objective lens. The laser

Table 1 Influence of laser scan speed on the resistivity. Laser power: 2.5 W, scan spacing: 50 μm

Precursor film	Scan speed (mm/s)	Surface resistivity (Ω/sq) after laser sintering	Thickness (nm)
Ag nanoparticle film from 5 wt% sol.	0.50	4.45×10^8	11.5
Ag nanoparticle film from 5 wt% sol.	5.00	6.30	8.5

sintering with the scan speed of 6.00 mm/s also gave a film with a low surface resistivity of 5.98 Ω/sq. The difference of the resistivity can be explained by the morphological difference of the films as shown in Fig. 7. The Ag film with the higher surface resistivity has an island structure as shown in Fig. 7a. On the other hand, the lower surface resistivity film prepared under the higher laser scan speed showed a network structure consisting of continuous branched silver micropatterns and holes. The formation of such a unique conductive network structure must be due to the rapid heating and quenching process caused by laser irradiation and the rapid scanning. The non-equilibrium process reduced the grain growth and inhibited the formation of discontinuous island structure.

The transmission spectra of the Ag nanoparticle films after sintering are shown in Fig. 8. In the case of conventional heat treatment, the lowest Ag nanoparticle concentration of spin-coating solution which gives a conductive silver thin film after sintering is ca. 10 wt%. The transparency of the film in visible region is lower than 10 % as shown in Fig. 8a. With the decreasing concentration from 10 to 5 wt%, the transparency increased as shown in Fig. 8b, however, the film was almost an insulator. On the other hand, the laser sintering of the Ag nanoparticle film from 5 wt% solution gave a conductive film as shown in Table 1 and then showed high transparency in the UV region. The transparency in visible region also increased higher than 20 %.

The laser scan spacing during the laser sintering as defined by Fig. 2 also influenced the surface resistivity significantly. As shown in Fig. 2, the length of the line-shaped beam is ca. 400 μm, there are overlappings between laser scan lines. In these experiments,

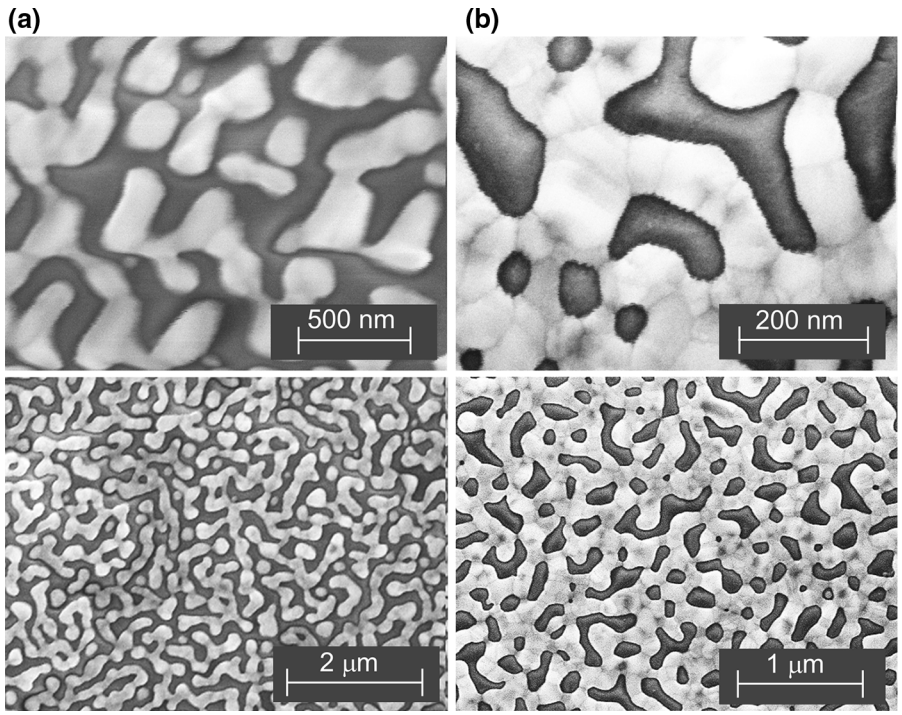

Fig. 7 SEM images of Ag nanoparticle films from 5 wt% solution after laser sintering. Scan speed: **a** 0.50 and **b** 5.00 mm/s

the scan speed was set to 0.5 mm/s, which is the condition similar to that of the high resistivity film in Table 1, to emphasize the influences of scan spacing on the surface resistivity. The images of laser beam scanning with different scan spacings of 50, 100, 200, and 300 μm where the length of line-shaped beam is 400 μm are schematically illustrated in Fig. 9. When the scan spacing is 50 μm, the line-shaped laser beam scans on the same area 8 times because the width of the first scan line is 400 μm and the shift of the laser beam at the next scan is 50 μm. By the estimation based on the length of the line-shaped beam (400 μm) and the scan spacing, the numbers of scan times on the same area with the scan spacing of 50, 100, and 200 μm are 8, 4, and 2, respectively, as shown in Fig. 9. When the scan spacing is 300 μm, the overlapping width of the first scan with the next scan is 100 μm and the overlapping is partial at the both side of the laser-scanned line as shown in Fig. 9d.

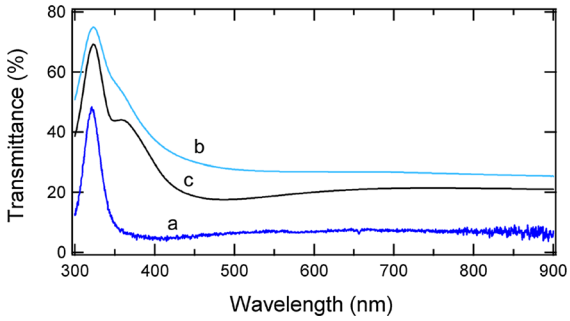

Fig. 8 Transmission spectra of silver thin films. *a* Ag nanoparticle film from 10 wt% solution after heat treatment at 300 °C for 30 min in air, *b* Ag nanoparticle film from 5 wt% solution after heat treatment at 300 °C for 30 min in air, and *c* Ag nanoparticle film from 5 wt% solution after laser sintering (scan speed: 5.00 mm/s, scan spacing: 50 μm, laser power: 2.5 W)

Table 2 shows the influences of scan spacing on the surface resistivity of Ag films. The surface resistivity decreased with increasing in the scan spacing. The lowest surface resistivity of 12.2 Ω/sq was obtained with the scan spacing of 300 μm. When the scan spacing decreased from 300 to 200 μm, the surface resistivity remarkably increased to be 3.23×10^3 Ω/sq. The morphological changes caused by the overlapping of laser-irradiated lines were investigated as shown in Fig. 10, where the laser beam was scanned on the same line by changing the overwrite time. In the experiments, the scan speed was set to 1.00 mm/s to emphasize the influences of overwrite time on the morphological changes. With increasing the overwrite time, the SEM image showed the narrowing of the network structure and the decreasing of the contacting points. Such morphological changes caused by multiple scan of laser beam explain the increase of the surface resistivity with decreasing in the scan spacing.

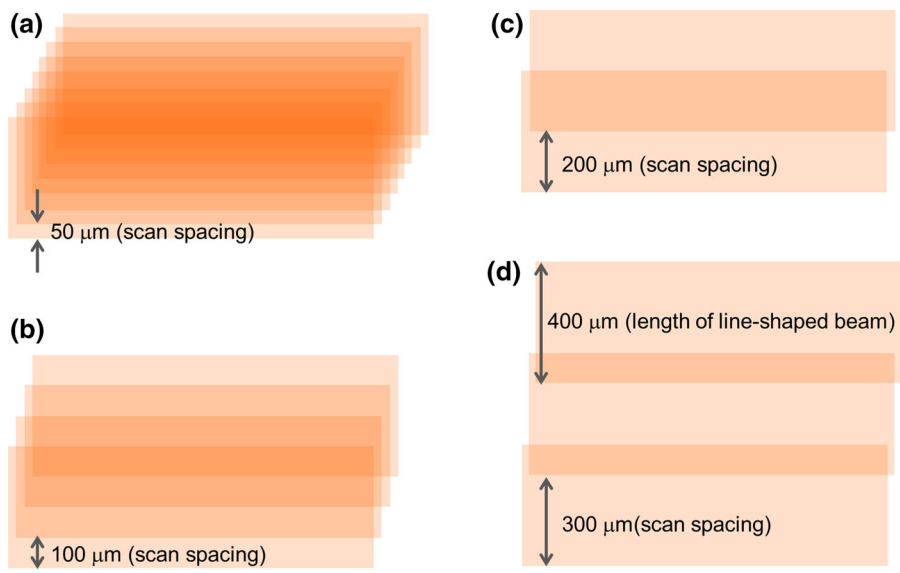

Fig. 9 Images of laser beam scanning with different scan spacing of **a** 50, **b** 100, **c** 200, and **d** 300 μm. Length of line-shaped beam: 400 μm

Table 2 Influences of scan spacing on the surface resistivity of Ag films. Laser power: 2.5 W, scan speed: 0.50 mm/s

Precursor film	Scan spacing (μm)	Surface resistivity (Ω/sq) after laser sintering
Ag nanoparticle film from 5 wt% sol.	50	4.45×10^8
Ag nanoparticle film from 5 wt% sol.	100	7.43×10^7
Ag nanoparticle film from 5 wt% sol.	200	3.23×10^3
Ag nanoparticle film from 5 wt% sol.	300	12.2

Influences of the addition of Cu nanoparticles

To increase the transparency in the visible region, the further decrease of film thickness is necessary; however, the lowest limit of the Ag nanoparticle concentration of the spin-coating solution which gives a conductive thin film is ca. 5 wt% even by the laser sintering. The film from 3 wt% solution showed insulation after laser sintering. As one of the factors to reduce the grain growth and increase the homogeneity of a silver thin film, the interaction between a silver layer and a substrate can be considered. Cu nanoparticles were added to the Ag nanoparticle solutions to enhance the interaction, and then Cu-doped Ag nanoparticle films were prepared by spin-coating. In the case of the Cu nanoparticle, the partial oxidation of the nanoparticle is caused by the sintering in air. In previous paper, we have studied the laser sintering of Cu nanoparticle film in air (Watanabe et al. 2007). A conductive Cu thin film can be prepared by laser sintering, although the film sintered by conventional heat treatment in air was almost an insulator. The conductivity of the laser-sintered Cu thin film depended on the laser scan speed, where the higher conductive film was obtained with the higher scan speed. This result could be explained by considering the competing processes, oxidation and fusion of Cu nanoparticles. The scan speed dependence of the conductivity also suggests that the surface of the Cu nanoparticle is oxidized even by the laser sintering. When such a partially oxidized Cu nanoparticles are doped in the Ag thin film, the interaction between the copper oxide and hydroxyl groups of a glass substrate can be expected as illustrated in Fig. 11.

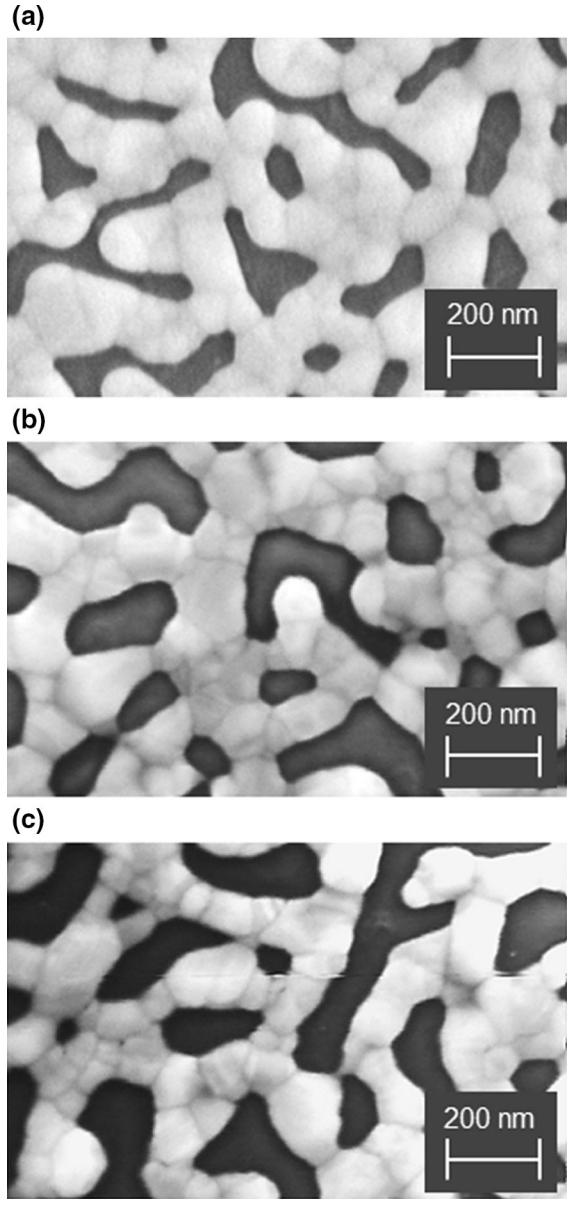

Fig. 10 SEM images of Ag nanoparticle films from 5 wt% solution after laser sintering. Scan speed: 1.00 mm/s, laser power: 2.5 W, overwrite time: **a** 1, **b** 2, and **c** 3

Figure 12 shows the SEM images of Cu-doped Ag nanoparticle films from 5 wt% solution (Ag/Cu = 95/5) after laser sintering by changing the scan spacing of the laser beam. The surface resistivities of the films are summarized in Table 3. By adding Cu nanoparticles to the Ag thin film, the surface resistivity was lowered to 2.40 Ω/sq. As shown in Fig. 12c, the SEM image of the film with the lowest resistivity shows a dense

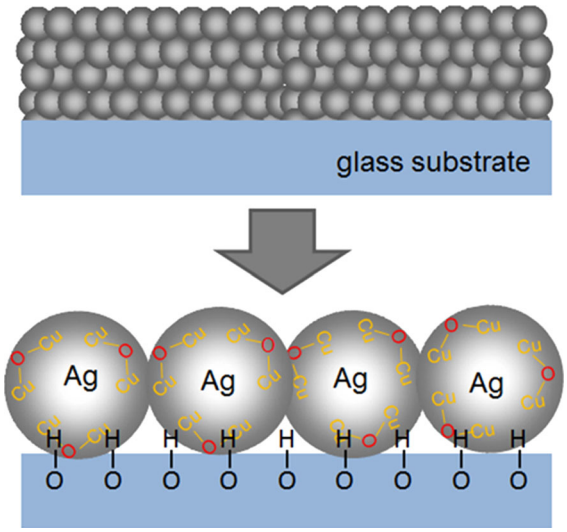

Fig. 11 Image of the enhancement in the interaction between Ag nanoparticles and a glass substrate by adding Cu nanoparticles during sintering

network structure compared with that of the pure Ag thin film as shown in Fig. 7. In addition, the dependence of the morphology on the scan spacing is not remarkable. Even with the narrowest scan spacing of laser beam (50 μm), the network structure was continuous and the surface resistivity was low enough (26.7 Ω/sq) although the pure Ag thin film gave a high surface resistivity by laser sintering with the same scan spacing (50 μm) as shown in Table 2. Such improvement of the conductivity can be explained by considering the increase of the interaction between the partially oxidized Cu nanoparticles and a glass substrate as illustrated in Fig. 11. The chemical structure of the Cu-doped Ag film was studied by micro-Raman spectroscopy. The typical Raman band assigned to oxides was observed as shown in Fig. 13. The Raman bands of Cu_2O (297, 411, 492, 633, and 786 cm^{-1}) and CuO (250, 300, 347, and 635 cm^{-1}) have been reported (Hamilton et al. 1986; Maoa et al. 2012).

Figure 14 shows the transmission spectra of Cu-doped Ag nanoparticle films from 5 wt% solution (Ag/Cu = 95/5) after laser sintering. The film as shown in Fig. 14a shows the highest transparency in the visible region, which can be attributed to the network

Table 3 Influences of scan spacing on the resistivity of the Cu-doped Ag films. Laser power: 2.5 W, scan speed: 5.00 mm/s

Ag/Cu in film	Total wt% of nanoparticles in spin-coating solution	Line spacing (μm)	Surface resistivity (Ω/sq)
95/5	5	50	26.7
95/5	5	100	2.67
95/5	5	300	2.40

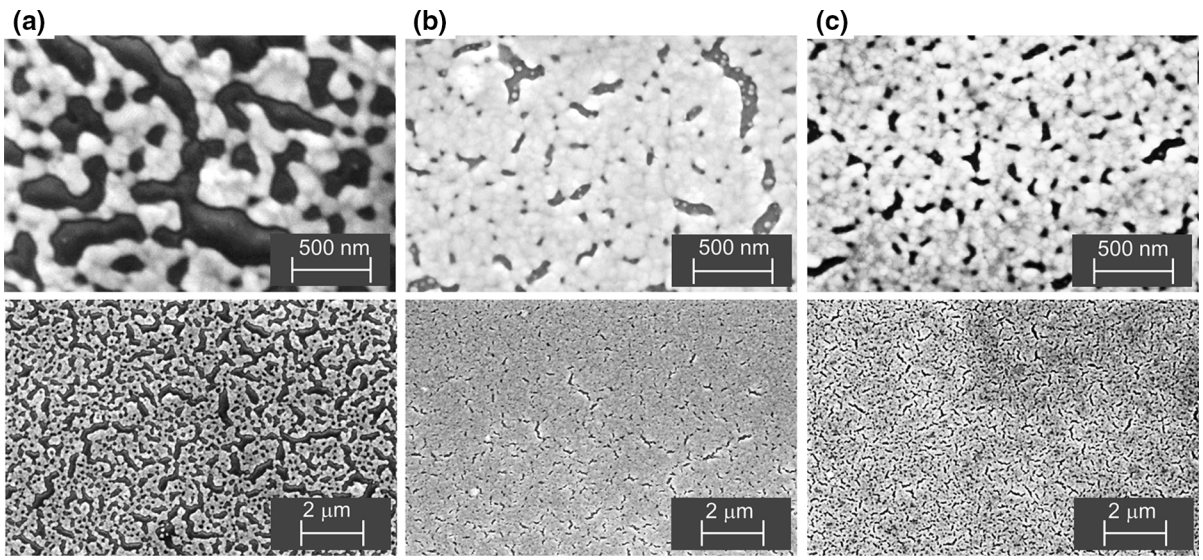

Fig. 12 SEM images of Cu-doped Ag nanoparticle films from 5 wt% solution (Ag/Cu = 95/5) after laser sintering. Scan speed: 5.00 mm/s, laser power: 2.5 W, scan spacing: **a** 50, **b** 100, and **c** 300 μm

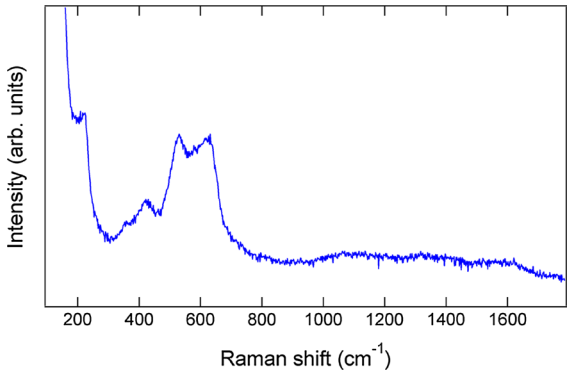

Fig. 13 Raman spectrum of Cu-doped Ag nanoparticle film from 5 wt% solution (Ag/Cu = 95/5) after laser sintering. Scan speed: 5.00 mm/s, laser power: 2.5 W, scan spacing: 300 μm

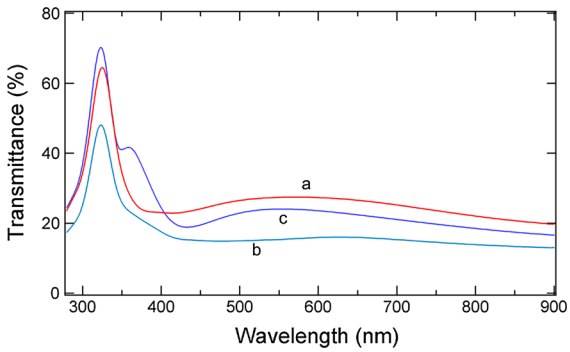

Fig. 14 Transmission spectra of Cu-doped Ag nanoparticle films from 5 wt% solution (Ag/Cu = 95/5) after laser sintering. Scan speed: 5.0 mm/s, laser power: 2.5 W, scan spacing: *a* 50, *b* 100, and *c* 300 μm

structure consisting of an island structure and holes. The laser sintering of the Cu-doped Ag nanoparticle films prepared from the further lower nanoparticles concentration was carried out and the conductivities are summarized in Table 4. The concentration could be decreased to 3.0 wt% keeping the surface resistivity lower than 10 Ω/sq with increasing the weight ratio of Cu nanoparticles to 15 % (Ag/Cu = 85/15). In the experiments, the scan speed of the laser beam was set to 2.0 mm/s because the sintering did not take place at the higher scan speed (5.0 mm/s) due to the lower absorption of laser energy by the thinner precursor film. The transparency of the film was increased higher than 20 % in the visible region as shown in Fig. 15, whereas the transparency in the UV region is lower

Table 4 Influences of Cu content on the resistivity of the Cu-doped Ag films. Laser power: 2.5 W, scan speed: 2.00 mm/s, scan spacing: 200 μm

Total nanoparticle concentration (wt%) in spin-coating solution	Ag/Cu in film	Surface resistivity (Ω/sq)
4.0	95/5	17.5
3.0	95/5	3.85×10^5
3.0	85/15	5.85

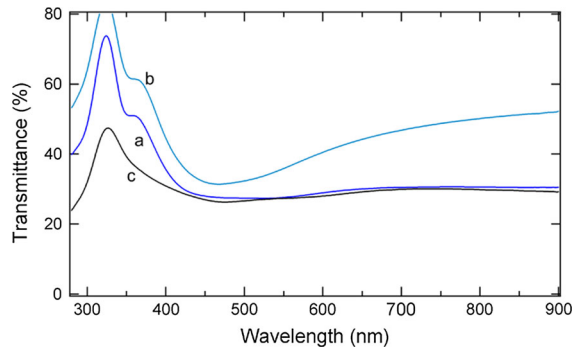

Fig. 15 Transmission spectra of Cu-doped Ag nanoparticle films from after laser sintering. Scan speed: 2.00 mm/s, laser power: 2.5 W, scan spacing: 200 mm. Total nanoparticle concentration (wt%) in spin-coating solution and the Ag/Cu ratio are *a* 4.0 and 95/5, *b* 3.0 and 95/5, *c* 3.0 and 85/15, respectively

than that of a pure Ag film, which can be attributed to the absorption of copper.

Conclusions

Laser sintering was an effective method to fabricate a conductive thin film by a wet process using Ag nanoparticle ink. The scan of the line-shaped laser beam (CW DPSS laser, 1,064 nm) on the Ag nanoparticle film gave a conductive thin film with a unique network structure. The laser-sintered Ag thin film showed a high transparency in UV region. The scan speed of the laser beam remarkably influenced the morphology and the conductivity of the laser-sintered thin film. With increasing the scan speed from 0.50 to 5.00 mm/s, the surface resistivity decreased from 4.45×10^8 to 6.30 Ω/sq. The addition of Cu nanoparticles to Ag thin film was also studied to improve

the homogeneity of the film and the conductivity based on the interaction between the oxidized Cu nanoparticle and a glass substrate. By adding Cu nanoparticles to the Ag thin film, the surface resistivity was lowered to 2.40 Ω/sq.

Acknowledgments This work was partially supported by JSPS KAKENHI under Grant Number 24360301 and also by MEXT KAKENHI under Grant Number 24102004. The authors thank Mr. Masao Ishii for the assistance in the FE-SEM measurements.

References

Aminuzzaman M, Watanabe A, Miyashita T (2008a) Fabrication of silver microwiring on a double-decker shaped polysilsesquioxane film by laser direct writing. J Photopolym Sci Technol 21(4):537–540

Aminuzzaman M, Watanabe A, Miyashita T (2008b) Photochemical surface modification and characterization of double-decker-shaped polysilsesquioxane hybrid thin films. J Mater Chem 8:5092–5097

Aminuzzaman M, Watanabe A, Miyashita T (2010) Direct writing of conductive silver micropatterns on flexible polyimide film by laser-induced pyrolysis of silver nanoparticle-dispersed film. J Nanopart Res 12:931–938

Arnold CB, Serra P, Piqué A (2007) Laser direct-write techniques for printing of complex materials. MRS Bull 32(1):23–31

Atsuki T, Hayashi T, Kiyoshima R, Oda M (2004) Metal nanoparticle and method for producing same, liquid dispersion of metal nanoparticle and method for producing same, metal thin line, metal film and method for producing same. PCT/JP2004/012968

Auyeung RCY, Kim H, Birnbaum AJ, Zala-lutidinov M, Mathews SA, Piqué A (2009) Laser decal transfer of freestanding microcantilevers and microbridges. Appl Phys A 97:513–519

Auyeung R, Kim H, Charipar N, Birnbaum A, Mathews S, Piqué A (2011) Laser forward transfer based on a spatial light modulator. Appl Phys A Mater Sci Proc 102(1):21–26

Choi TY, Poulikakos D, Grigoropoulos CP (2004) Fountain-pen-based laser microstructuring with gold nanoparticle inks. Appl Phys Lett 85(1):13–15

Fuller SB, Wilhelm EJ, Jacobson JM (2002) Ink-jet printed nanoparticle microelectromechanical systems. J Microelectromech Syst 11(1):54–60

Gamerith S, Klug A, Scheiber H, Scherf U, Moderegger E, List EJW (2007) Direct ink-jet printing of Ag–Cu nanoparticle and Ag-precursor based electrodes for OFET applications. Adv Func Mater 17(6):3111–3118

Jeong S, Song HC, Lee WW, Lee SS, Choi Y, Son W, Kim ED, Paik CH, Oh SH, Ryu BH (2011) Stable aqueous based Cu nanoparticle ink for printing well-defined highly conductive features on a plastic substrate. Langmuir 27(6):3144–3149

Hamilton JC, Farmer JC, Anderson RJ (1986) In situ raman spectroscopy of anodic films formed on copper and silver in sodium hydroxide solution. J Electrochem Soc 133(4):739–745

Kim H, Kushto GA, Arnold CB, Kafa ZH, Piqué A (2004) Laser processing of nanocrystalline TiO_2 flms for dye-sensitized solar cells. Appl Phy Lett 85(3):464–466

Kim H, Auyeung RCY, Piqué A (2007) Laser-printed thick-film electrodes for solid-state rechargeable Li-ion microbatteries. J Power Sources 165(1):413–419

Kim H, Melinger J, Khachatrian A, Charipar N, Auyeung R, Piqué A (2010) Fabrication of terahertz metamaterials by laser printing. Opt Lett 35(23):4039–4041

Ko H, Pan H, Grigoropoulos CP, Luscombe CK, Fréchet JMJ, Poulikakos D (2007a) Air stable high resolution organic transistors by selective laser sintering of ink-jet printed metal nanoparticles. Appl Phys Lett 90:141103

Ko SH, Park I, Pan H, Grigoropoulos CP, Pisano AP, Luscombe KC, Fréchet JMJ (2007b) Direct nanoimprinting of metal nanoparticles for nanoscale electronics fabrication. Nano Lett 7(7):1869–1877

Ko SW, Chung J, Hotz N, Nam KH, Grigoropoulos CP (2010) Metal nanoparticle direct inkjet printing for low-temperature 3D micro metal structure fabrication. J Micromech Microeng 20:125010

Komatsu H (1991) Interferometry: principles and applications of two-beam and multiple beam interferometry. Nikon Tech Bull. http://www.tecnicaenlaboratorios.com/Nikon/Brochures/Technical%20Bulletin%20Interferometry%201991.pdf

Luechinger NA, Athanassiou EK, Stark WJ (2008) Graphene-stabilized copper nanoparticles as an air-stable substitute for silver and gold in low-cost ink-jet printable electronics. Nanotechnology 19:445201

Maoa Y, Hea J, Suna X, Li W, Lua X, Gana J, Liu Z, Gong L, Chen J, Liu P, Tonga Y (2012) Electrochemical synthesis of hierarchical Cu_2O stars with enhanced photoelectrochemical properties. Electrochim. Acta 62:1–7

Murata K, Matsumoto J, Tezuka A, Matsuba Y, Yokoyama H (2005) Super-fine ink-jet printing: toward the minimal manufacturing system. Microsyst Technol 12(1–2):2–7

Oda M, Katsu I, Tsuneizumi M, Fuchita E, Kashu S, Hayashi C (1992) Ultrafine particle films by gas deposition method. MRS Proc 286:121. doi:10.1557/PROC-286-121

Oda M, Abe T, Suzuki T, Saito N, Iwashige H, Kutluk G (2001) Application of dispersed nanoparticles. MRS Proc 704, W3.1.1. doi:10.1557/PROC-704-W3.1.1

Parka BK, Kima D, Jeonga S, Moona J (2007) Direct writing of copper conductive patterns by ink-jet printing. Thin Solid Films 515(19):7706–7711

Perelaer J, de Gans BJ, Schubert US (2006) Ink-jet printing and microwave sintering of conductive silver tracks. Adv Mater 18(16):2101–2104

Piqué A, Chrisey DB, Auyeung RCY, Fitz-Gerald J, Wu HD, McGill RA, Lakeou S, Wu PK, Nyuyen V, Duignan M (1999) A novel laser transfer process for direct writing of electronic and sensor materials. Appl Phys A 69:S279–S284

Piqué A, Auyeung R, Kim H, Metkus K, Mathews S (2008) Digital microfabrication by laser decal transfer. J Laser Micro/Nanoeng 3(3):163–169

Singh M, Haverinen HM, Dhagat P, Jabbour GE (2010) Inkjet printing-process and its applications. Adv Mater 22(6):673–685

Tamai T, Watanabe M, Hatanaka Y, Tsujiwaki H, Nishioka N, Matsukawa K (2008) Formation of metal nanoparticles on the surface of polymer particles incorporating polysilane by UV irradiation. Langmuir 24(24):14203–14208

Wang J, Auyeung R, Kim H, Charipar N, Piqué A (2010) Three-dimensional printing of interconnects by laser direct-write of silver nanopastes. Adv Mater 22(40):4462–4466

Watanabe A (2013) Laser sintering of metal nanoparticle film. J Photopolym Sci Technol 26(2):199–205

Watanabe A, Kobayashi Y, Konno M, Yamada S, Miwa T (2005) Direct drawing of Ag microwiring by laser-induced pyrolysis of film prepared from liquid-dispersed metal nanoparticles. Jpn J Appl Phys 44:L740–L742

Watanabe A, Kobayashi Y, Konno M, Yamada S, Miwa T (2007) Direct drawing of submicron wiring by laser-induced pyrolysis of film prepared from liquid-dispersed metal nanoparticles. Mol Cryst Liq Cryst 464:161–167

Watanabe A, Aminuzzaman M, Miyashita T (2009) Submicron writing by laser irradiation on metal nano-particle dispersed films towards flexible electronics. Proc SPIE 7202:6

Watanabe A, Cheng CW, Shen WC, Chu CI (2012) Fabrication of micropatterns by laser direct writing using nanomaterials. J Photopolym Sci Technol 25:679–680

Woo K, Kim D, Kim JS, Lim S, Moon J (2009) Ink-jet printing of Cu–Ag-based highly conductive tracks on a transparent substrate. Langmuir 25(1):429–433

Yonezawa T (2009) In-situ observation of silver nanoparticle ink at high temperature. Biomed Mater Eng 19(1):29–34

ULVAC Inc (2014) Nanometal Ink. http://www.ulvac.co.jp/products_e/materials/nano-metal-ink

Watanabe A, Miyashita T (2007) Formation of copper microwiring by laser direct writing. J Photopolym Sci Technol 20(1):115–116